($HC_2O_4^-$), the anion of threonoic acid (T^-), and O_2

$$A(O_2)^{-}\cdot + O_2^- \xrightarrow{H_2O} CH_2(OH)CH(OH)CH(OH)C(O)O^- + HC_2O_4^- + O_2 \quad (16)$$

The overall reaction is

$$A + 2O_2^- \rightarrow T^- + HC_2O_4^- + O_2 \quad (17)$$

Hence, in DMF O_2^- acts as a dioxygenase of dehydroascorbic acid via cleavage of its C_2, C_3 bond.

Combination of eq 14 and 17 yields an overall reaction whose stoichiometry is consistent with the experimental results when H_2A is limiting relative to O_2^- (the observed stoichiometry is $2.7O_2^-$ per H_2A).

$$3H_2A + 8O_2^- \rightarrow 3T^- + 3HC_2O_4^- + 3O_2 + 2OH^- \quad (18)$$

Under alkaline conditions HA^- reacts facilely with molecular oxygen in both aqueous and aprotic media. This represents another dimension of the unique ability of H_2A to serve as an antioxidant and protective agent from activated dioxygen species. On the basis of previous studies[6] and the observation of transient levels of O_2^- by ESR, a reasonable reaction sequence in alkaline DMF is

$$2O_2 + 2HA^- \rightarrow 2O_2^- + H_2A + A \quad (19)$$

$$2O_2^- + A \xrightarrow{H_2O} T^- + HC_2O_4^- + O_2 \quad (20)$$

The overall reaction has a stoichiometry of one dioxygen per ascorbate ion to give threonoate and oxalic acid.

$$O_2 + HA^- \rightarrow T^- + H_2C_2O_4 \quad (21)$$

Although oxidation and oxygenation of H_2A by O_2^- in DMF yields oxalate, which is consistent with the metabolic fate of H_2A in many plants,[20,21] a direct O_2^-–H_2A process in plant metabolism is unreasonable. However, a dioxygenase enzyme (possibly a copper protein) may activate O_2 in a manner to promote the chemistry of reactions 11–21. This proposition is under active investigation.

The present results confirm that ascorbic acid, its anion, and dehydroascorbic acid are unique in their ability to destroy superoxide ion without the production of reactive intermediate radicals. Especially noteworthy is that one H_2A molecule can deactivate more than 2.5 superoxide ions. However, the production of oxalate, which results from such a stoichiometry, probably does not occur under most biological conditions because ascorbic acid usually occurs at concentrations that are at least three orders of magnitude greater than superoxide ion. When O_2^- is limiting, eq 11–13 will prevail; thus, the most hazardous product from ascorbic acid deactivation of superoxide ion is dehydroascorbic acid and hydrogen peroxide; under alkaline conditions HA^- destroys H_2O_2.

Work in progress is directed to the effect of transition-metal complexes on the activation of O_2, O_2^-, and H_2O_2 for reaction with H_2A and A. Some of this chemistry may prove relevant to the in vivo mechanism of oxidation and oxygenation of H_2A to oxalate in plants.[20,21]

Acknowledgment. This work was supported by the National Science Foundation under Grant No. CHE79-22040 and by the University of California Agricultural Experiment Station under Project No. CA-R-BPS-4080. We are grateful to Dr. Der-Hang Chin of this department and to Professor Henry Po of the California State University at Long Beach for assistance with the stopped-flow kinetic measurements.

Registry No. H_2A, 50-81-7; HA^-, 299-36-5; A^-, 34481-26-0; A, 490-83-5; A_2, 72691-25-9; $A(O_2)^-$, 83313-12-6; T^-, 83313-10-4; $HC_2O_4^-$, 920-52-5; O_2^-, 12185-08-9; H_2O_2, 7722-84-1; benzoquinone, 106-51-4; 2,3-diketogulonic acid anion, 83313-11-5; δ-gluconolactone, 90-80-2.

Porphyrins. 43.† Triplet Sublevel Emission of Platinum Tetrabenzoporphyrin by Spectrothermal Principal Component Decomposition

Thijs J. Aartsma,‡ Martin Gouterman,* Clemens Jochum, Alvin L. Kwiram, Barry V. Pepich, and Loren D. Williams‡

Contribution from the Department of Chemistry, University of Washington, Seattle, Washington 98195. *Received February 9, 1982*

Abstract: The synthesis and absorption spectra are reported for Pt^{II}(TBP) (peaks at 394 and 595 nm) and for $Pt^{IV}(TBP)X_2$ (peaks at 417 and 619 nm) (TBP = tetrabenzoporphyrin). The former shows strong phosphorescence at 745 nm with a quantum yield in degassed pyridine at room temperature of 0.18 ± 0.04; the latter is dark. The phosphorescence spectrum and lifetime of Pt(TBP) vary in the temperature range 4–84 K, but all decays are exponential. The decay rates are fitted with the assumption of thermal equlibrium among three triplet levels: Two levels at energy E_1 have an average decay rate $\bar{k}_1 = (418\ \mu s)^{-1}$; a third level at energy E_3 has a decay rate $k_3 = (22\ \mu s)^{-1}$; $E_3 - E_1 = 22.6\ cm^{-1}$. The temperature-dependent emission spectra are studied by principal component analysis, which shows two distinct spectra are present. These two spectra are determined within narrow limits. From the spectral decomposition we also determine the ratio $2\bar{k}_{1r}/k_{3r} = 0.0369$, where $\bar{k}_{1r}$ is the average radiative decay rate for the lower two levels and k_{3r} is that of the third level, and obtain an independent estimate that $E_3 - E_1 = 22.7\ cm^{-1}$.

Recently Vogler et al.[1] reported the synthesis and optical spectra of palladium and platinum tetrabenzoporphyrin (TBP). The relation between the spectra of the reported Pd(TBP) and Pt(TBP) was contrary to the known relation between the spectra in the porphyrin series.[2,3] In the porphyrin series the change Pd → Pt is characterized by a blue shift to the optical absorption and emission and an enhancement of the phosphorescence intensity. For the tetrabenzoporphyrin reported by Vogler et al., the change Pd → Pt gave rise to a red shift of the optical absorption and emission and a strong decrease in phosphorescence emission. This

† Part 42: Rawlings, D. C.; Davidson, E. R.; Gouterman, M. *Theor. Chim. Acta* **1982**, *61*, 227.

‡ Present addresses: T.J.A., Department of Chemistry, Florida State University, Tallahassee, FL 32306; L.D.W. Department of Chemistry, Duke University, Durham, NC 27706.

(1) Vogler, A.; Kunkely, H.; Rethwisch, B. *Inorg. Chim. Acta* **1980**, *46*, 101.
(2) Eastwood, D.; Gouterman, M. *J. Mol. Spectrosc.* **1970**, *35*, 359.
(3) Buchler, J. W.; Lay, K.-L.; Stoppa, H. *Z. Naturforsch.* **1980**, *35b*, 433.

0002-7863/82/1504-6278$01.25/0

Table I. Wavelength (nm) and Absorbance Ratios for Principal Maxima for Metallotetrabenzoporphyrins[a]

molecule	$B(0,0)$	$Q(1',0)$	$Q(1,0)$	$Q(0,0)$	ref
Pt(TBP)	394, 0.97	540, 0.09	581, 0.10	595, 1.00	*b*
Pd(TBP)	407, 1.00	558, 0.04	584, 0.06	607, 0.48	1
$Pt(TBP)X_2$	417, 1.00	568, 0.04	594, 0.05	619, 0.38	*b*
Zn(TBP)	432, 1.00	582, 0.03	602, 0.02	628, 0.32	15

[a] In pyridine except Pd(TBP) in DMF. [b] This paper.

surprising result prompted us to reinvestigate the synthesis of Pt(TBP). As reported herein we have obtained another species, which we believe is properly identified as Pt(TBP).

Considerable interest arises in Pt(TBP). The phosphorescence yield of platinum etioporphyrin has been reported to be 0.9.[2] This suggests potential use of this material as a luminescent solar concentrator for photovoltaic devices.[4] However, the lowest energy absorption band of platinum etioporphyrin is at 536 nm, and so it is transparent to much of the visible solar spectrum. Pt(TBP) might be expected to absorb more to the red yet have a comparably high phosphorescence yield. As reported herein, these expectations are partially obeyed.

Beyond the above two issues, the sublevel zero-field splitting of the emitting ^3E_u state in Pt(TBP) is of interest. This splitting has been studied experimentally and theoretically in Pt(P) (P = porphine) by the van der Waals group,[5-7] and it is valuable to see how this splitting occurs in the tetrabenzoporphyrin ring. The van der Waals group, working with the quasiline spectra of Pt(P) in octane crystals at low temperature, deduced the zero-field splitting of the ^3E_u state from the structure of the absorption $^3E_u \leftarrow {}^1A_{1g}$ (monitored in excitation spectra) and from the effect of magnetic fields on the quasiline absorption and emission spectra. In this paper we use a cruder sample, i.e., Pt(TBP) in pyridine snow. We use the temperature dependence of the lifetime to determine the zero-field splitting, a technique developed by Crosby and co-workers.[8] In addition we have applied principal component analysis to the temperature-dependent emission spectra.[9] This method has been previously applied to fluorescence analysis,[10] to mass spectral data,[11] and to absorption spectra.[12] As applied to the present problem it allows us to show that two independent spectra account for the various observed phosphorescence spectra; furthermore, within certain limits the independent spectra are derived, and a second estimate of the energy gap between the emitting sublevels is obtained. Principal component decomposition does not seem to have been previously applied to the triplet sublevel problem.

Experimental Section

Synthesis and Absorption Spectra. Zn(TBP) was prepared by the template method of Vogler[13] and demetalated to H_2(TBP) with sulfuric acid by the procedure described in ref 1. Over a period of 48 h, 0.1 g of crude H_2(TBP) was slowly added to a refluxing solution of 0.2 g of $PtCl_2$ in 125 mL of benzonitrile by use of a Soxhlet extractor. This follows the method used by Buchler to insert platinum into free base tetra-*p*-tolylporphyrin (TTP).[3] The procedure yields a product with an absorption spectrum of a metallotetrabenzoporphyrin. We identify the product as Pt(TBP), i.e., the Pt^{II} species. The product was purified by flash chromatography using toluene containing the minimal amount of pyridine required to allow the chromatography to proceed. The absorption spectrum of the purest sample, taken on a Cary 219 spectrophotometer, is shown in Figure 1. Upon excitation with light of wavelength 595 nm at 77 K, the product showed a strong emission at 747 nm. An excitation spectrum of this emission band was taken on a Perkin-Elmer 650-10S spectrofluorimeter. This excitation spectrum showed the principal bands listed in Table I; however, the broad absorption, shown in Figure 1 between 406 and 526 nm, was missing. We have assumed that the product obeys the customary rules of emission spectroscopy and have used the excitation spectrum to correct the observed absorption spectrum to provide a true spectrum of the product Pt(TBP) shown in Figure 1.

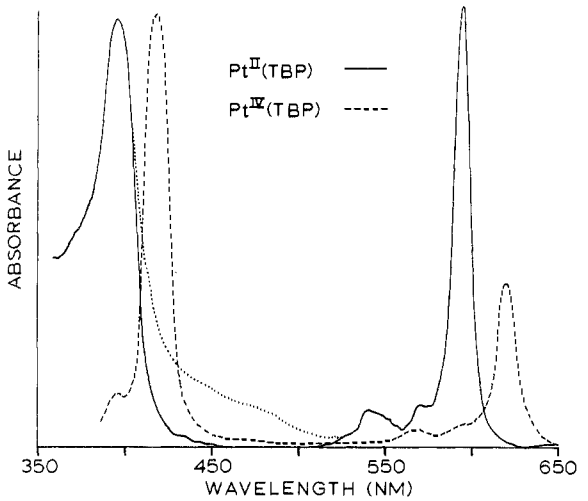

Figure 1. Solid line: Absorption spectrum of Pt^{II}(TBP) in pyridine at room temperature. (From 406 to 526 nm the observed absorption spectrum is the dotted line, which is corrected to the solid line by reference to the excitation spectrum. See text.) Dashed line: Observed absorption spectrum of $Pt^{IV}(TBP)X_2$ in pyridine. (Produced by Br_2 oxidation. See text.)

That the product of our synthesis is Pt(TBP) is based on several arguments. Firstly, there is the mode of synthesis. Secondly, the absorption and emission of the species is blue shifted from that of Pd(TBP),[1] as expected from the shift observed between the spectra of palladium and platinum porphyrins.[2,3] Moreover, the phosphorescence is quite intense. A quantum yield was measured at room temperature in degassed pyridine, and a value of 0.18 ± 0.04 was obtained.[4] Such high quantum yields are fully consistent with the behavior of platinum(II) porphyrins.[2] As discussed below, further confirmation is obtained from the behavior on oxidation and from mass spectroscopic data. Finally, we have the low-temperature emission behavior, described below, that closely parallels the behavior of Pt(P).

Before describing the oxidation of Pt(TBP), we should discuss the comparable findings of Buchler on the oxidation of platinum(II) to platinum(IV) porphyrin.[3] Quite generally the spectrum of a platinum(IV) porphyrin lies between that of the strongly blue-shifted platinum(II) porphyrin and that of zinc porphyrin.[3] This is explained by reduced back-bonding of the filled metal $e_g(5d_\pi)$ orbitals with the ring LUMO orbitals $e_g(\pi^*)$; less back-bonding is expected since the energy of the $5d_\pi$ should be lower in Pt^{IV} than in Pt^{II}.[3,14] Furthermore, $Pt(TTP)Cl_2$ prepared by Buchler was examined for emission, and none was found.[15] Iterative extended Hückel calculations on $Pd(P)Cl_2$ provided an explanation for this finding,[15] since this molecule is found to have a low-energy empty $a_{1g}(d_{z^2})$ orbital. Hence the lack of emission of platinum(IV) porphyrin can be rationalized by the presence of forbidden (π,d_{z^2}) charge-transfer states between the lowest energy $^3(\pi,\pi^*)$ levels and the ground state, a condition that generally leads to quenching of emission.[14,15]

Pt(TBP) was oxidized by bubbling $Br_2(g)$ through a solution in pyridine. The reaction was carried out in an absorption cell; a transfer pipet was used to add gaseous Br_2. A new spectrum was observed with peaks between those of Pt(TBP) and those of Zn(TBP)[16] (Figure 1 and Table

(4) Offenhartz, P. O'D.; Micheels, R. H.; Darrow, A. D. SERI Progress Report, Newton, MA, April 1981, Subcontract XW-0-8041-13.
(5) Noort, M.; Jansen, G.; Canters, G. W.; van der Waals, J. H. *Spectrochim. Acta, Part A* **1976**, *32A*, 1371.
(6) Van Dijk, N.; Noort, M.; Voelker, S.; Canters, G. W.; van der Waals, J. H. *Chem. Phys. Lett.* **1980**, *71*, 415.
(7) Devolder, P.; van Dijk, N.; Thijssen, H. P. H., van der Waals, J. H. *Mol. Phys.* **1981**, *43*, 335.
(8) Crosby, G. A. *Acc. Chem. Res.* **1975**, *8*, 231.
(9) Davis, John L. "Statistics and Data Analysis in Geology"; Wiley: New York, 1973.
(10) Warner, I. M.; Christian, G. D.; Davidson, E. R.; Callis, J. B. *Anal. Chem.* **1977**, *49*, 564.
(11) Sharaf, M. A.; Kowalski, B. R. *Anal. Chem.* **1981**, *53*, 518.
(12) Gold, H. S.; Rasmussen, G. T.; Mercer-Smith, J. A.; Whitten, D. G.; Buck, R. P. *Anal. Chim. Acta* **1980**, *122*, 171.
(13) Vogler, A.; Kunkely, H. *Angew. Chem., Int. Ed. Engl.* **1978**, *17*, 760.
(14) Gouterman, M. In "The Porphyrins"; Dolphin, D., Ed.; Academic Press: New York, 1978; Vol. III, Chapter 1, p 1.
(15) Antipas, Artemis Ph.D. Thesis, University of Washington, Seattle, WA, 1979.
(16) Edwards, L.; Gouterman, M.; Rose, C. B. *J. Am. Chem. Soc.* **1976**, *98*, 7638.

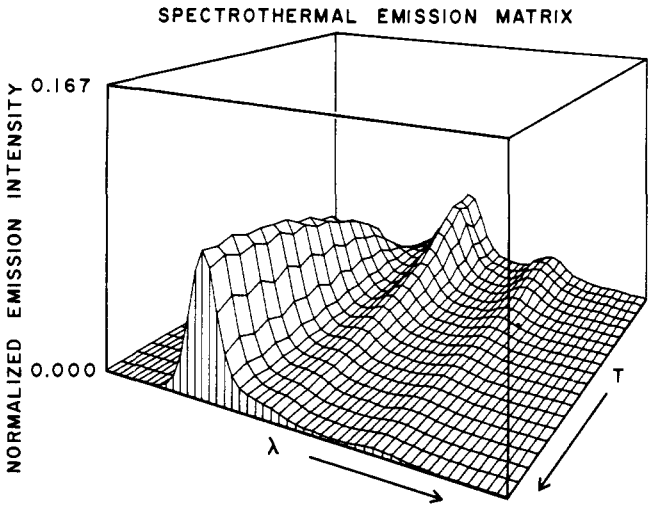

Figure 2. Normalized emission spectra are plotted as a function of temperature. The wavelengths, λ_j, are equally spaced from 716 to 814 nm; the temperatures, T_i, are unequally spaced, lying between 3.8 and 29.6 K.

I). Excitation at the 619-nm absorption peak in a pyridine solution at 77 K showed no emission. Upon addition of hydrazine hydrate the species reverted to Pt(TBP). This evidence is totally consistent with the expected behavior of a Pt^{IV} species. However, it is not clear whether the ligands are Br atoms or, perhaps, OH from residual water. So we identify the compound as $Pt(TBP)X_2$, i.e., the Pt^{IV} species. The spectrum reported in Table I for $Pt(TBP)X_2$ compares well with that previously reported as "Pt(TBP)" by Vogler and Kunkely,[1] and it is reasonable to suppose that this is the identity of the previously reported species.

Mass Spectra. All mass spectra acquired in this study were taken on a Hewlett-Packard HP 5985 GC/MS data system equipped with a thermal desorption direct insertion probe.[17] All samples were injected via a 10-μL syringe onto a Pt wire (0.2-mm diameter) from which the samples were thermally desorbed after the solvent had been evaporated. A power supply using a Variac and a filament transformer allowed the Pt resistor to heat to temperatures in excess of 600 °C in a few seconds.

Our purified Pt(TBP) was examined as described above. Clear mass peaks stand out at 702, 703, and 704 u, the three principal peaks expected for the compound. We also took a mass spectrum of the "Pt(TBP)" kindly supplied by Professor Vogler. No ions were seen in the 703-μ region. However, a weak group of peaks was seen around 352 u, which corresponds to $Pt(TBP)^{2+}$; other weak peaks were observed around 431 u, which corresponds to $[Pt(TBP)Br_2]^{2+}$.

It should be noted that a sample of Pd(TBP), also provided by Professor Vogler, was run on the mass spectrometer at the University of British Columbia courtesy of Dr. Paul Smith and Professor David Dolphin. It showed a strong parent peak, thus confirming its identification.

Low-Temperature Spectroscopic and Kinetic Measurements. For the investigation of the spectroscopy and phosphorescence lifetimes of Pt(TBP), we used a solution of this compound in pyridine, which occasionally formed a glass on cooling down to 4.2 K but generally was a snow at these temperatures. The lifetime measurements and the phosphorescence spectra as a function of temperature were obtained by inserting the sample in a liquid helium cryostat for optical spectroscopy. The temperature was controlled by slowly cooling the sample with cold helium gas. Alternatively, starting at 4.2 K the Dewar would warm up sufficiently slowly to permit data acquisition at a well-defined temperature. The temperature was measured with a Lakeshore Cryotronics diode, and electronic readout was calibrated to an accuracy of 0.1 K. Typically, the temperature changed less than 0.5 K during the recording of a spectrum of a decay curve. Data acquisition was facilitated by the extensive use of a PDP-8 microcomputer.

The phosphorescence spectra were obtained with a 0.25-m Jarrell Ash spectrometer, set for 2-nm resolution. Another Jarrell Ash monochromator with a xenon lamp was used for excitation at 592 nm. Filters were used where appropriate. The spectra were recorded by photon counting for a certain period at each wavelength step and subsequently stored in digital format for later analysis. Figure 2 shows the variation of the phosphorescence spectrum as a function of temperature. The spectra in this figure have been normalized to unit area. The actual integrated phosphorescence intensity increased by a factor of about four between

(17) Bruins, A. P. *Anal. Chem.* **1980**, *52*, 605.

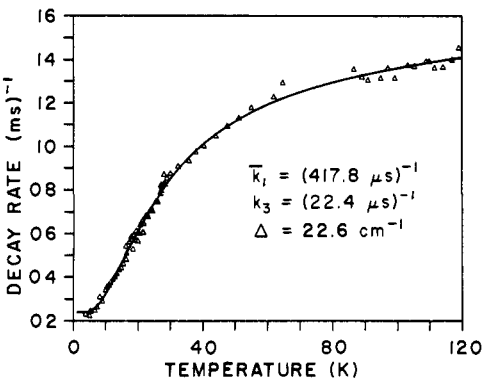

Figure 3. Triangles are experimental decay rates. The solid line is fitted to eq 11 with the parameters indicated.

4 and 100 K. However, since the integrated phosphorescence intensity is subject to instabilities in the system, the spectra were normalized for the principal component decomposition.

The phosphorescence lifetimes were measured with a transient recorder (Biomation, Model 805) with a time resolution down to 200 ns. The sample was excited with a nitrogen-laser-pumped dye laser at 592 nm corresponding to the lowest excited singlet state of Pt(TBP). The phosphorescence was monitored at 746 nm through a 0.25-m Jarrell Ash monochromator with a cooled EMI 9558 photomultiplier tube. At temperatures below 8 K we also measured lifetimes at 764 nm, the maximum of the phosphorescence intensity for this temperature range. The results at 746 and 764 nm, however, were essentially identical. The detection sensitivity was increased by feeding the output of the photomultiplier into a fast preamplifier (rise time 1 μs) prior to the transient recorder.

The data analysis was done with the departmental VAX computer system. A standard least-squares fitting routine based on a finite difference Levenberg–Marquardt algorithm[18] was used to fit the decaying curves to a single exponential. A second method, using a program developed by S. W. Provencher,[19,20] gave essentially the same results. The second method did not require an initial guess and had the considerable advantage of being able to analyze multiple-component decay curves. All the decay curves for temperatures below ~100 K fitted accurately to single exponentials. At higher temperatures we observe a multiexponential behavior, which we attribute to quenching effects possibly due to increased mobility. (Such increased mobility might give nonexponential decay, for example by oxygen quenching, since the samples were not degassed.) In Figure 3 we plot the exponential decay rates observed as a function of temperature.

Principal Component Decompsition

The triplet state of a porphyrin consists of several sublevels 1, ... q, ... s. (The number s is not necessarily 3 if there is orbital degeneracy or if we are dealing with a tripmultiplet.[14]) We wish to determine the number of independent emitting levels and their spectra. We shall consider an $m \times n$ emission matrix $\mathbf{V} = [v_{ij}]$; here i labels temperature T_1, ... T_i, ... T_m and j labels wavelength λ_1, ... λ_j, ... λ_n. In our principal component decomposition we used $m = 20$ and $n = 50$. This matrix can be expressed in terms of the spectra of the individual sublevels:

$$v_{ij} = \sum_{q=1}^{s} x_i^{(q)} y_j^{(q)} \tag{1}$$

Here $y_j^{(q)}$ is the emission spectrum of sublevel q at wavelength λ_j, which we assume is independent of temperature; $x_i^{(q)}$ is the fractional contribution of spectrum q to the observed spectrum at temperature T_i. We normalized all spectra to unit area:

$$\sum_j v_{ij} = 1 \qquad \sum_j y_j^{(q)} = 1 \tag{2}$$

It then follows from (1) and (2) that the $x_i^{(q)}$ are normalized as

$$\sum_{q=1}^{s} x_i^{(q)} = 1 \tag{3}$$

It is useful to introduce some vector notation:

(18) Brown, K. M.; Dennis, J. E. *Numerishe Mathematik* **1972**, *18*, 289.
(19) Provencher, S. W. *Biophys. J.* **1976**, *16*, 27.
(20) Provencher, S. W. *J. Chem. Phys.* **1976**, *64*, 2772.

$$\mathbf{v}_i = [v_{i1}, v_{i2}, \ldots v_{in}] \quad (4a)$$

$$\mathbf{y}^{(q)} = [y_1^{(q)}, y_2^{(q)}, \ldots y_n^{(q)}] \quad (4b)$$

Thus $\mathbf{v}_i$ represents the observed emission spectrum at temperature T_i, and $\mathbf{y}^{(q)}$ is the emission spectrum of sublevel q; both are normalized to unit area.

Linear principal component analysis[9-12] shows that the number of independent emitting levels q in the summation of eq 1 is equal to the number of nonzero eigenvalues of the square matrix $\mathbf{V}^t\mathbf{V}$, where $\mathbf{V}^t$ is the transpose of $\mathbf{V}$. In our case we find two principal nonzero eigenvalues, whose orthonormal eigenvectors we call $\mathbf{v}^A$ and $\mathbf{v}^B$; note that the normalization here is $\sum_j (v_j^A)^2 = 1$. These two vectors are plotted in Figure 4. The individual observed spectra can then be expressed as

$$\mathbf{v}_i = \alpha_i \mathbf{v}^A + \beta_i \mathbf{v}^B \quad (5)$$

In our case $\mathbf{v}^A$ and $\mathbf{v}^B$ express 99.72% (85.16% and 14.56%, respectively) of the total variance of the measured spectra. (This is determined from the ratio of the nonzero eigenvalues of $\mathbf{V}^t\mathbf{V}$ to the trace of $\mathbf{V}^t\mathbf{V}$.) Since the measured spectra always contain some noise and the computations are subject to round-off errors, it is reasonable to assume that the remaining 0.28% of the total variance are due to those effects. The (α_i,β_i) in eq 5 are determined by the inner products

$$\alpha_i = (\mathbf{v}^A,\mathbf{v}_i) \qquad \beta_i = (\mathbf{v}^B,\mathbf{v}_i) \quad (6)$$

The various calculated values (α_i,β_i) are plotted in Figure 5 and lie along line G. (See Appendix.)

We now consider the spectra of the individual sublevels. Since there are only two basis vectors, only two sublevel spectra can be determined. We will call these

$$\mathbf{y}^{(0)} = \alpha^{(0)}\mathbf{v}^A + \beta^{(0)}\mathbf{v}^B$$

$$\mathbf{y}^{(1)} = \alpha^{(1)}\mathbf{v}^A + \beta^{(1)}\mathbf{v}^B \quad (7)$$

The following constraints enter into the determination of $(\alpha^{(0)}, \beta^{(0)})$ and $(\alpha^{(1)}, \beta^{(1)})$: (i) The entries of $\mathbf{y}^{(0)}$ and $\mathbf{y}^{(1)}$ must be nonnegative. (ii) The observed spectra v_i must be linear combinations of the $\mathbf{y}^{(q)}$, i.e.,

$$\mathbf{v}_i = x_i^{(0)}\mathbf{y}^{(0)} + x_i^{(1)}\mathbf{y}^{(1)} \quad (8)$$

with the $x_i^{(q)}$ nonnegative.

As shown in the Appendix, the second constraint requires that the solutions $(\alpha^{(0)}, \beta^{(0)})$ and $(\alpha^{(1)}, \beta^{(1)})$ lie on the extension of line G beyond the points A_2 and B_2 (Figure 5) set by the extreme (α_i, β_i) values. The first constraint confines the solutions for eq 7 to the region between the points with labels A_1 and B_1. With these constraints we can construct boundaries for the pure spectra $y^{(0)}$ and $y^{(1)}$ in Figure 6; the uncertainty in the values for $(\alpha^{(0)}, \beta^{(0)})$ and $(\alpha^{(1)}, \beta^{(1)})$ is shown by the shaded areas. From eq 3, 5, 7, and 8 we can also derive an expression for ratio of the fractional intensities:

$$x_i^{(0)}/x_i^{(1)} = (\alpha^{(1)} - \alpha_i)/(\alpha_i - \alpha^{(0)}) \quad (9a)$$

$$x_i^{(0)} + x_i^{(1)} = 1 \quad (9b)$$

[An equivalent expression holds among β_i, $\beta^{(0)}$, $\beta^{(1)}$; however, insofar as the points (α_i, β_i) lie on a straight line, the β formula gives results identical with those of the α formula.] The point $(\alpha^{(0)}, \beta^{(0)})$ was chosen to coincide with point A_2 (Figure 5), since it seemed reasonable to postulate that only the lowest energy sublevel contributed to the lowest temperature emission spectra. The point $(\alpha^{(1)}, \beta^{(1)})$ was chosen to lie midway between points B_2 and B_1 (Figure 5). With these choices, a plot of the $x_i^{(0)}$ and $x_i^{(1)}$ is made in Figure 7.

Empirical Fit for the Zero-Field Splitting

Porphyrins in D_{4h} symmetry have lowest triplet, ^3E_u, which has a 6-fold degeneracy. Some time ago two of the authors[21] discussed the zero-field splitting of the six levels caused by three terms: H_{so} (spin–orbit coupling), H_{cf} (environmental crystal field), and H_{ss} (spin–spin coupling). More recently the effect of an external magnetic field was also included.[6] For our present study we can omit the external magnetic field and the small H_{ss} terms. Following eq 7 of ref 6 we obtain six energies displaced from the average as follows:

$$E_{1,2} = -(1/2)(Z^2 + \delta^2)^{1/2} = -(\delta/2) - \Delta \quad (10a)$$

$$E_3 = -\delta/2 \quad (10b)$$

$$E_4 = \delta/2 \quad (10c)$$

$$E_{5,6} = (1/2)(Z^2 + \delta^2)^{1/2} = (\delta/2) + \Delta \quad (10d)$$

Here Z is the spin–orbit coupling integral, δ is the crystal field

(21) Gouterman, M.; Yamanashi, B. S.; Kwiram, A. L. *J. Chem. Phys.* **1972**, *56*, 4073.

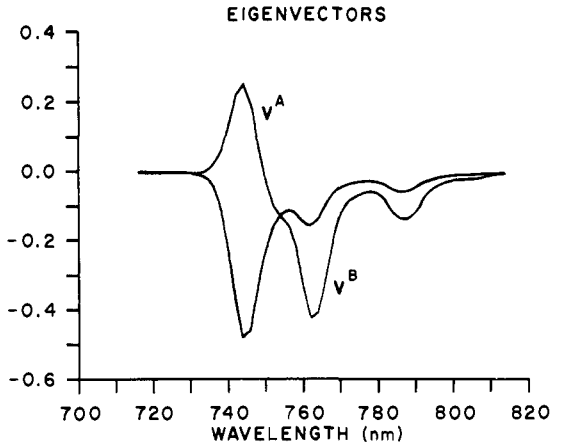

Figure 4. Normalized spectral eigenvectors.

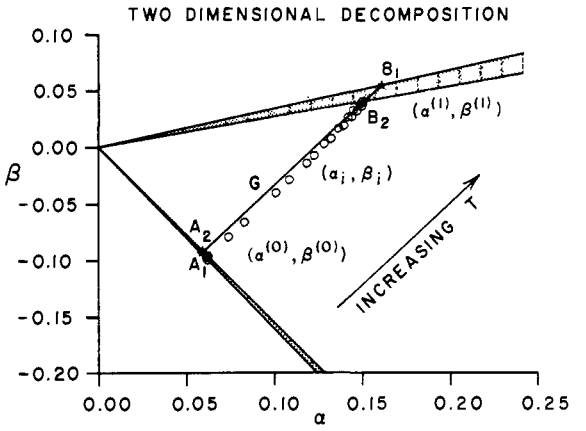

Figure 5. The coefficients (α_i, β_i) for the various temperatures T_i.

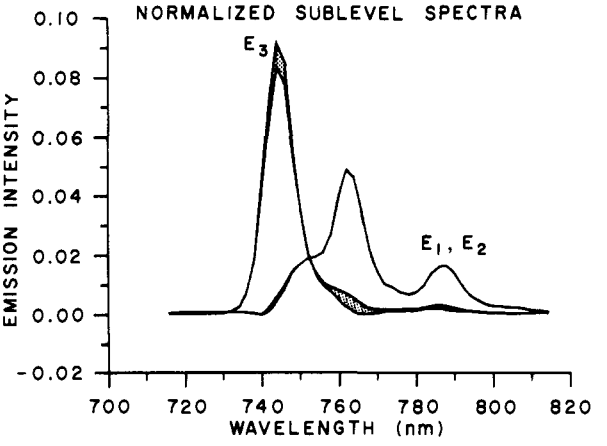

Figure 6. The two resolved normalized sublevel spectra. The E_i label the zero-field levels E_1, E_2, and E_3. Shaded area shows uncertainty in the analysis.

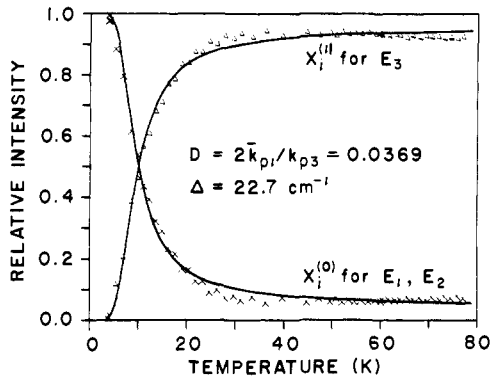

Figure 7. The relative normalized emission intensity of the zero-field levels E_1, E_2, and E_3. The heavy solid lines are fitted to eq 14 with the parameters indicated.

splitting, and Δ is defined for convenience. In D_{4h} symmetry the levels 1, 2, 5, and 6 have space-spin symmetry $\mathcal{A}_{1u}$, $\mathcal{A}_{2u}$, $\mathcal{B}_{1u}$, $\mathcal{B}_{2u}$, while the levels 3 and 4 have symmetry $\mathcal{E}_u$. (The script letters signify space-spin symmetry.) The crystal field will cause the $\mathcal{E}_u$ levels to split into two levels, $\mathcal{E}_{u\xi}$ and $\mathcal{E}_{u\eta}$. The axes of polarization of these levels will depend on the direction of the crystal field. The crystal field will also couple the levels $\mathcal{A}_{1u}$, $\mathcal{A}_{2u}$, $\mathcal{B}_{1u}$, $\mathcal{B}_{2u}$, with the detailed coupling dependent on the crystal field orientation. The zero-field splitting of the ^3E_u state is shown in Figures 1 of ref 6 and 7. The emission origin of levels 1, 2, 5, and 6 is very weak and out-of-plane polarized; the emission origin of levels 3 and 4 is much stronger and in-plane polarized.

For our spectral fits we shall consider only levels 1, 2, and 3. Since the emission decay was well fitted by a single exponential, we assume thermal equilibrium among the sublevels. We follow the earlier treatments and take levels 1 and 2 as degenerate;[6,7] because of thermal equilibrium their kinetic parameters appear as an average. Under these assumptions the triplet decay rate, k_t, is given by

$$k_t = (2\bar{k}_1 + k_3 e^{-\Delta/kT})/(2 + e^{-\Delta/kT}) \tag{11}$$

Here $\bar{k}_1$ is the average decay rate of levels 1 and 2; k_3 is the decay rate of level 3; and Δ is the activation energy from eq 9. The rate of photon emission from these sublevels is as follows:

$$d(P_1 + P_2)/dt = 2\bar{k}_{1r}N_1 \tag{12a}$$

$$dP_3/dt = k_{3r}N_3 \tag{12b}$$

$$N_3/N_1 = e^{-\Delta/kT} \tag{12c}$$

The dP_i/dt are the photon emission rates of levels i; $\bar{k}_{1r}$, is the average radiative emission rate for levels 1 and 2; k_{3r} is the radiative emission rate for level 3; and the N_i are the populations of level i. Going back to the definitions in eq 1 and the conclusion (eq 8) that only two spectra are observed, we can deduce that

$$x_i^{(0)}/x_i^{(1)} = 2\bar{k}_{1r}/k_{3r}e^{-\Delta/kT_i} = De^{\Delta/kT_i} \tag{13}$$

(See Appendix for a small correction to eq 13.) From eq 9b and 13, we can deduce the following empirical forms for the fractional emission intensities:

$$x_i^{(0)} = D/(D + e^{-\Delta/kT_i}) \tag{14a}$$

$$x_i^{(1)} = e^{-\Delta/kT_i}/(D + e^{-\Delta/kT_i}) \tag{14b}$$

Equation 11 was used to fit the observed decay rates plotted in Figure 3. The fitted curve, represented by the solid line in Figure 3, agrees quite well with the experimental results. The best least-squares fit was obtained with parameters:

$$\bar{k}_1 = (417.8\ \mu s)^{-1} \qquad k_3 = (22.4\ \mu s)^{-1}$$
$$\Delta = 22.6\ cm^{-1} \tag{15}$$

Equations 14a and 14b were used to fit the fractional emission intensities. The solid lines in Figure 7 represent the best least-squares fit to the data with parameters:

$$D = 2\bar{k}_{1r}/k_{3r} = 0.0369 \qquad \Delta = 22.7\ cm^{-1} \tag{16}$$

Thus the activation energy, Δ, agrees well by the two methods.

Further Refinements

Some attempts were made to take into account the effect of the higher levels 4, 5, and 6 in the least-squares fitting routine, but the experimental results were not accurate enough to allow any conclusion to be drawn from these calculations: The resulting fits were hardly any better than those obtained from the three-level model. The effect of the levels 4, 5, and 6 should be small, since these levels are 70 cm^{-1} above levels 1, 2, and 3 in the case of Pt(P) in octane[6] and a comparable or larger energy gas is expected for Pt(TBP) in pyridine.

Another refinement concerns the very low temperature data. A slight negative dip can be seen in the spectra of sublevels E_1 and E_2 at 740 nm in Figure 6. This dip may arise from the fact that there are two lowest energy levels, which have not been resolved. Principal component analysis of the four lowest temperature emission spectra suggests that there are three components in the spectra, as expected theoretically. Presumably, if more very low temperature data were available, we could establish the existence of two separate levels E_1 and E_2 rather than treat them as an average.

Conclusions and Comparisons

This paper shows that the spectral relations among palladium and platinum tetrabenzoporphyrins parallels those observed in porphyrins: In particular the transition energy decreases in the order $Pt^{II} > Pd^{II} > Zn^{II}$. Moreover, for both porphyrin and tetrabenzoporphyrin, the Pt^{II} complex shows a very strong triplet emission, while Pt^{IV}, at least on first examination, is dark.

Our spectral studies have included study of the zero-field splitting of the emitting, 6-fold degenerate ^3E_u state in Pt(TBP) in pyridine. We have used a method different from that applied to Pt(P) in octane:[5-7] Our method is based on analysis of the temperature variation of the lifetime and the broad-band spectrum, while that applied to Pt(P) was based on temperature and magnetic field effects on quasiline spectral data.

Our conclusions about the ^3E_u state generally agree with those found on Pt(P). Both our lifetime and principal component decomposition agree that there are two distinct emitting levels. We identify the lower level as the lowest energy degenerate pair predicted by the theory of the ^3E_u state.[6,7,21] We identify the upper level as that component of the ^3E_u ($S_z = 0$) level shifted to lower energy by the crystal field. The levels remain in thermal equilibrium over the temperature range 4–100 K, as judged by the single exponential decay shown by the phosphorescence. In agreement with the findings on Pt(P),[6,7] the lower level shows a slow decay time of 418 μs while the upper level shows a faster decay time of 22 μs. The emission spectra of the two levels shows markedly different vibronic structure: The highest energy emission peak of the lower level is weak while that of the upper level is strong. This is consistent with their predicted space-spin symmetry: The lower level is a mixture of symmetries $\mathcal{A}_{1u}$, $\mathcal{A}_{2u}$, $\mathcal{B}_{1u}$, $\mathcal{B}_{2u}$ while the upper level is $\mathcal{E}_{u\xi}$. Thus the origin band of the lower level should have out-of-plane polarization, while the origin band of the upper level can borrow intensity from the strong in-plane (π,π^*) transitions, as discussed elsewhere.[6,7,21,22] The lifetime analysis and principal component decomposition agree on the energy gap between the two levels, $\Delta = 22 \pm 1$ cm^{-1}. This value for Pt(TBP) in pyridine compares to 16.5 cm^{-1} reported for Pt(P) in octane.[6] This quantity Δ is related to the spin–orbit coupling, Z, and the crystal-field splitting, δ, as

$$\Delta = (1/2)[(Z^2 + \delta^2)^{1/2} - \delta] \tag{17}$$

It should be noted that Crosby and co-workers not only analyzed emission lifetimes by eq 11, but they also provided a method to analyze triplet emission spectra.[8,23,24] While their method allows

(22) Ake, R. L.; Gouterman, M. *Theor. Chim. Acta* **1969**, *15*, 20.
(23) Baker, D. C.; Crosby, G. A. *Chem. Phys.* **1974**, *4*, 428.
(24) Fordyce, W. A.; Rau, H.; Stone, M. L.; Crosby, G. A. *Chem. Phys. Lett.* **1981**, *77*, 405.

determination of the energy gap between two emitting levels, the method of principal component decomposition used here has several additional features: (i) In the case of two sublevels, within certain limits we determine the emission spectrum of each sublevel. (ii) Because we work with the entire spectrum, we also determine the ratio of the radiative decay rates (eq 13 and Appendix), which was not obtainable by the Crosby method that uses just two wavelengths. (iii) Finally, the method of principal component decomposition provides a simple procedure for deciding the number of independent sublevel spectra. Thus the method applied here for analyzing the temperature dependence of triplet sublevel emission spectra should be more generally applicable to such problems, which occur in a variety of molecular systems.

Acknowledgment. This research was supported by NSF Grant DMR-7823958 and by the Office of Naval Research. We thank Professor Arndt Vogler of the Universität Regensberg for sending us tetrabenzoporphyrin samples and Dr. Paul Smith and Professor David Dolphin of the University of British Columbia for running mass spectra of them. Professor Bruce Kowalski gave encouragement in the principal component analysis. James Van Zee provided valuable assistance with the computer programs. We thank Dr. Peter O'D. Offenhartz of EIC Laboratories, Newton, MA, for his unpublished quantum yield measurements. We also thank Infomatrix, Inc., for use of their principal component/curve resolution program, which obtained Figures 2 and 4–6. This program is available from Infomatrix, Inc., Seattle, WA 98125.

Appendix. Mathematical Addenda

(1) That the points (α_i, β_i) should lie on a line can be seen by summing over the entries in the vectors in eq 5. We have

$$\sum_j v_{ij} = 1 \qquad \sum_j v_j^{\mathrm{A}} = A \qquad \sum_j v_j^{\mathrm{B}} = B \tag{18}$$

Hence, from eq 5,

$$1 = A\alpha_i + B\beta_i \tag{19}$$

Use of the same procedure on eq 7 and 8 shows that the points $(\alpha^{(0)}, \beta^{(0)})$ and $(\alpha^{(1)}, \beta^{(1)})$ must lie on the extensions of the same line.

(2) Because the emission spectra were uncorrected for the wavelength dependence of the detector sensitivity, eq 13 needs a correction. The emission matrix v_{ij} can be expressed as

$$v_{ij} = \sum_{q=1}^{s} k_{q\mathrm{r}} D_j f_j^{(q)} N_q(T_i) \Big[\sum_j \sum_{q=1}^{x} k_{q\mathrm{r}} D_j f_j^{(q)} N_q(T_i)\Big]^{-1} \tag{20}$$

where $k_{q\mathrm{r}}$ is the radiative emission rate of level q, $f_j^{(q)}$ is the normalized emission spectra of sublevel q expressed as photons per unit wavelength, D_j is the detector sensitivity at wavelength λ_j, and $N_q(T_i)$ is the number of molecules in sublevel q at temperature T_i. The normalized uncorrected sublevel emission spectra are then defined as

$$y_j^{(q)} = D_j f_j^{(q)} \Big[\sum_j D_j f_j^{(q)}\Big]^{-1} \tag{21}$$

where the normalizing factors

$$u_q \equiv \sum_j D_j f_j^{(q)} \tag{22}$$

will not, in general, be identical for all sublevels q. Substitution of eq 21 and 22 into eq 20 yields

$$v_{ij} = \sum_{q=1}^{s} u_q k_{q\mathrm{r}} y_j^{(q)} N_q(T_i) \Big[\sum_{q=1}^{s} u_q k_{q\mathrm{r}} N_q(T_i)\Big]^{-1} \tag{23}$$

The fractional contribution of level q to the observed spectrum at temperature T_i then becomes

$$x_i^{(q)} = u_q k_{q\mathrm{r}} N_q(T_i) \Big[\sum_{q=1}^{s} u_q k_{q\mathrm{r}} N_q(T_i)\Big]^{-1} \tag{24}$$

Equation 24 leads to a modified form of eq 13

$$x_i^{(0)}/x_i^{(1)} = (2u_1 \bar{k}_{1\mathrm{r}}/u_3 k_{3\mathrm{r}}) e^{\Delta/kT_i} \tag{13'}$$

Since the emission spectra are in the same wavelength region, we expect that the correction factor $u_1/u_3 \sim 1$.

Registry No. Pt(TBP), 73797-39-4.

Cyclohexaamylose Complexation with Organic Solvent Molecules

Robert I. Gelb, Lowell M. Schwartz,* Michael Radeos, Robert B. Edmonds, and Daniel A. Laufer

Contribution from the Department of Chemistry, University of Massachusetts, Boston, Massachusetts 02125. *Received March 16, 1982*

Abstract: Weak inclusion complexes have been discovered between cyclohexaamylose (α-cyclodextrin) and several organic species (ethanol, 2-propanol, 2-methyl-2-propanol, cyclohexanol, dioxane, dimethyl sulfoxide and phenol) in aqueous solution. Formation constants for these complexes were determined by measuring the effect of the complexation on the pH of a cyclohexaamylose/acid/base buffer equilibrium. Enthalpies and entropies of complexation are calculated from the temperature dependences of the formation constants. The existences of true complexes were verified by (1) observing that these thermodynamic parameters correlate in the same manner as has been shown for other cyclohexaamylose complexes and (2) noting the similarities of ^{13}C NMR resonance behavior to that of well-established complexes.

In recent years there have appeared many reports of complexes of cycloamyloses and their derivatives with a wide variety of substrate species. Of the several experimental methodologies employed in these studies, those based on pH potentiometry have been particularly successful in terms of accuracy and convenience. In this laboratory we have used pH potentiometry to measure cycloamylose complexation constants of numerous aqueous organic acids, phenols and anions.[1-3] Other workers[4,5] have also utilized pH potentiometry similarly. Although the methodology has been

(1) Gelb, R. I.; Schwartz, L. M.; Johnson, R. F.; Laufer, D. A. *J. Am. Chem. Soc.* **1979**, *101*, 1869–1874.
(2) Gelb, R. I.; Schwartz, L. M.; Laufer, D. A. *Bioorg. Chem.* **1980**, *9*, 450–461.

0002-7863/82/1504-6283$01.25/0